Editorial

Remote Sensing Perspectives on Geomorphology and Tectonic Processes

Zhikun Ren [1,*], Peizhen Zhang [2], Takashi Oguchi [3] and Zhongtai He [4]

[1] State Key Laboratory of Earthquake Dynamics, Institute of Geology, China Earthquake Administration, Beijing 100029, China

[2] School of Earth Science and Geological Engineering, Sun Yat-Sen University, Guangzhou 510275, China; zhangpeizhen@mail.sysu.edu.cn

[3] Center for Spatial Information Science, University of Tokyo, Tokyo 113-0033, Japan; oguchi@csis.u-tokyo.ac.jp

[4] National Institute of Natural Hazards, Ministry of Emergency Management of China, Beijing 100085, China; hezhongtai@126.com

[*] Correspondence: rzk@ies.ac.cn

Abstract: The quantity and quality of remote sensing measurements of tectonic deformation have increased dramatically over the past two decades, improving our ability to observe active geomorphological tectonic processes. High-precision and high-resolution topography is the basis for the quantitative study of active geomorphological and tectonic processes. Recently, with the rapid development of computer visual science and the growing application of light detection and ranging (LiDAR), small unmanned aerial vehicles (UAVs) and structure from motion (SfM) photogrammetry have shown great potential in providing high-resolution and high-precision topographic information. In this Special Issue, we focus on the tectonic activity of active faults and the geomorphic processes in various global tectonic regimes that are related to remote sensing measurements. This Special Issue covers major earthquake hazards and seismogenic structures, new methods in seismological studies using high-resolution data sets, and the tectonic and geomorphic application of high-resolution data sets worldwide and, in particular, in the Eastern Tibetan Plateau and Tian Shan. These contributions will provide new insights into the remote sensing perspectives of geomorphological and tectonic processes.

1. Introduction

Geomorphology and tectonic processes are both important for understanding the geological history of the Earth. This history involves the origins and evolution of geomorphology and tectonic processes ranging from short-term to long-term deformations, which are multidisciplinary research topics involving geomorphology, tectonophysics, and earthquake geology. Research on the evolution of the tectonic geomorphology of plateau margins and orogenic belts usually focuses on the long term. Geomorphological features form gradually and repeat when morphogenic earthquakes are involved. The link between short-term and long-term geomorphic evolution is critical to understanding the evolution of tectonic geomorphology. Because of its recent development, remote sensing technology has gradually become the traditional method used to study geomorphological and tectonic processes. In particular, the availability of high-resolution data sets from satellite optical remote sensing, InSAR, aerial remote sensing, high-resolution drone airborne optical images, and LiDAR, coupled with advanced processing techniques and algorithms, has enabled us to better understand the interplay among crustal deformation, earthquake ruptures, and their signatures in geomorphic evolution.

We wrote this Special Issue to gather recent contributions concerning both short-term and long-term deformations that address the evolution of geomorphology and tectonic processes, particularly those that use remote sensing data. This Special Issue is part of the section titled "Remote Sensing in Geology, Geomorphology and Hydrology". Below,

we aim to study active tectonic geomorphological processes using high-resolution data acquired by different remote sensing platforms and sensors.

This Special Issue was organized by Guest Editors Zhikun Ren, Peizhen Zhang, Takashi Oguchi, and Zhongtai He, and they have engaged in active tectonic studies for many years [1–10].

In this paper, we compile 12 manuscripts that advance the understanding of active tectonics linked to strike-slip, normal, and thrust faults worldwide. These articles cover a wide range of topics, including major earthquake hazards, active tectonics, tectonic and geomorphic evolution, coseismic liquefaction using multisource data integration (e.g., satellite remote sensing, InSAR, high-resolution drone airborne optical images, and LiDAR; Figure 1), multiscale approaches focused on geomorphological and tectonic processes, and precise dating methods.

The published papers may be classified into the following groups.
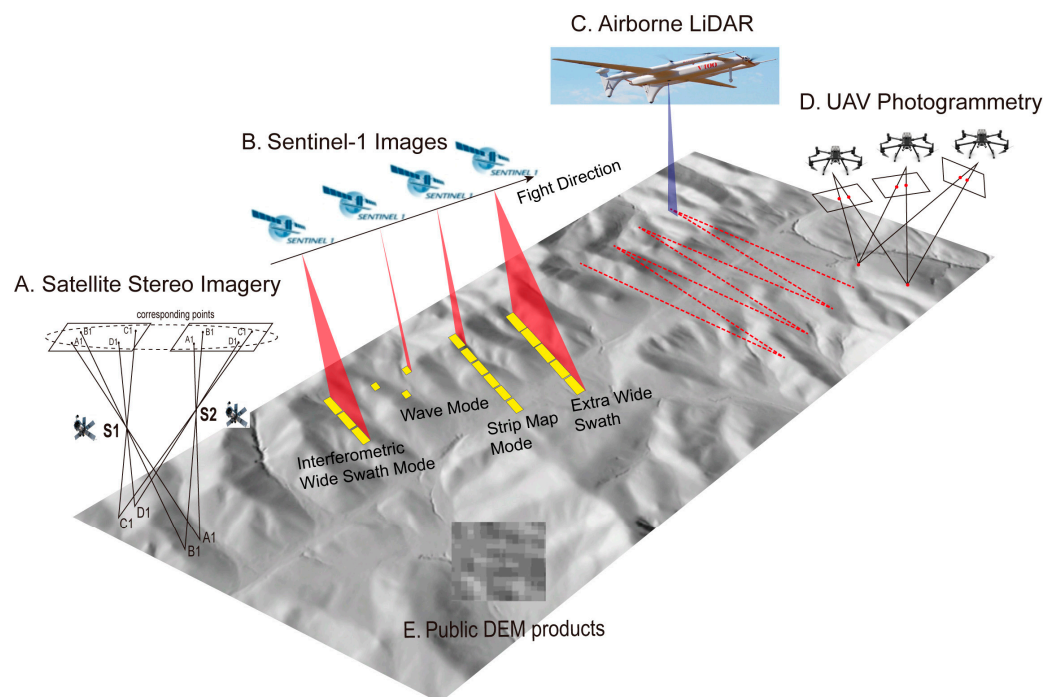

Figure 1. Multisource data integration discussed in this Special Issue. (**A**) Satellite stereo imagery; (**B**) InSAR sentinel-1 images; (**C**) airborne LiDAR; (**D**) UAV photogrammetry; (**E**) public DEM products.

2. Recent Major Earthquake Hazards and Seismogenic Structures

Earthquakes cause both the direct loss of life and property and can generate a series of secondary natural disasters and social impacts. During the time that this Special Issue was being processed, on 6 February 2023, strong earthquakes of magnitude 7.8 and 7.5 occurred in southcentral Turkey near the Turkish–Syrian border. Earthquake and aftershock records, as well as analyses by seismologists and tectonists, suggest that the two devastating earthquakes occurred in the East Anatolian Fault system, and they were both left-lateral strike-slip faults. These earthquakes are known as the 2023 Turkey Earthquake. It is rare to have two devastating earthquakes (magnitude 7.0+) occur within the same fault system, in the same area, and on the same day. Both earthquakes occurred on a continental plate. A dense population was present on the surface, which caused a great loss of life in the local area. Numerous houses collapsed, and roads and railways were severely damaged. The earthquakes occurred during a cold winter, and the rainfall that followed caused rescue difficulties and further casualties. China is also an earthquake-prone region. There are many different types of active structures with destructive seismic capabilities in the Chinese mainland and its adjacent areas, which face an extremely high risk of earthquake hazards.

An Mw 7.4 Maduo earthquake occurred on 22 May 2021 in the northern Qinghai–Tibet Plateau. The total length of the coseismic surface rupture is approximately 160 km. Multiple types of these rupture patterns exist, including linear shear fractures, obliquely distributed tensional and tensional–shear fractures, pressure ridges, and pull-apart basins. The earthquake also induced a large number of liquefaction structures and landslides in valleys and marshlands [11]. Within three days of the earthquake, Xie et al. [12] carried out high-resolution photography and topographical mapping of surface ruptures using unmanned aerial vehicle (UAV). The optical images were used to create a digital surface model (DSM) using the SfM technique and a set of ground control points collected with a real-time kinematic GPS. Combined with field observations, the detailed morphology of the surface rupture was obtained. The coseismic surface rupture extended in a WNW direction for ~160 km, with complicated geometry, along a relatively unknown young fault: the Jiangcuo Fault. Field surveys and detailed mapping revealed that the coseismic surface ruptures were characterized by a series of left-lateral offsets, en echelon tensional cracks and fissures, compressional mole tracks, and widespread sand liquefaction. The observed coseismic left-lateral displacements ranged from 0.2 m to ~2.6 m, while the vertical displacements ranged from 0.1 m to ~1.5 m. This study suggests that the multiple WNW-trending subfaults, including the Jiangcuo Fault, may be the subfaults of the East Kunlun Fault system bounding the Bayan Har Block. This would constitute a broad and dispersive northern boundary of the block, controlling the inner strain distribution and deformation.

On 8 January 2022, an Mw 6.7 earthquake struck Menyuan, Qinghai, China. The surface rupture is primarily a complex coseismic surface deformation zone formed by the combination of multiple types of faults, such as tensional fractures, tensional shear fractures, compression bulges, and seismic depressions, which are mainly characterized by sinistral strike-slip motion and, to a lesser extent, by thrusting. The earthquake caused severe damage to tunnel groups and line equipment in the Haomen–Junmachang section of the Lanzhou–Xinjiang high-speed railway, resulting in the suspension of the railway operation. The Mw 5.9 earthquake in 1986, the Mw 5.9 earthquake in 2016, and the Mw 6.7 earthquake in 2022 all occurred in the western section of the Lenglongling fault. Three strong earthquakes of more than M 6 occurred in a short period of time, indicating that this area is still an area where stress and deformation accumulate, which has the potential risk of large earthquakes [13,14]. To determine the rupture parameters of this event, Li et al. [15] mapped the coseismic InSAR deformation fields and further estimated the focal mechanism. In their study, the best-fitting solution emphasized that the 2022 Menyuan earthquake ruptured at the junction of the Tuolaishan fault and the Lenglongling fault. Both rupturing faults were dominated by a sinistral strike-slip, and the main slip was concentrated in the shallow part of the rupture plane. The maximum slip reached ~3.5 m, which occurred mainly at a depth of 4 km. The joint analysis of the optimal slip model, relocated aftershocks, Coulomb stress change, and field observations suggested that the strain energy in the Tuolaishan fault may not have been fully released and requires further attention.

After the 2022 Menyuan earthquake, Wang et al. [16] collected GF-7 and Sentinel-1 satellite images to measure the surface deformation of the earthquake sequence. The fault model and the fault slip distribution of the 2016 and 2022 Mengyuan earthquakes were inverted using coseismic surface displacements. The results show that the 2016 event was a reverse event, with the maximum coseismic surface displacement along the LOS reaching 8 cm. The surface rupture of the 2022 Mw 6.7 earthquake ran in the WNW–ESE direction, with a maximum displacement along the LOS of 72 cm. The main seismogenic fault of the 2022 event was the western segment of the Lenglongling fault. The Coulomb failure stress change suggests that the earthquake sequence around Menyuan was mainly governed by the activities of the Lenglongling fault around the northeastern Tibetan Plateau.

3. New Methods in Seismological Studies Using High-Resolution Data Sets

China's first optical stereo mapping satellite with a submeter resolution, GaoFen-7 (GF-7), which launched in November 2019, shows significant potential for providing high-resolution topographic and geomorphic data for quantitative research on active tectonics. For example, after the Menyuan Mw 6.7 earthquake on 8 January 2022, GF-7 satellite images were acquired that same day and revealed the overall distribution characteristics, structural style, and dislocation scale of the surface rupture, which provided an important reference for earthquake emergency response and field investigation [13,14,17]. However, no studies have evaluated the capability of the GF-7-generated digital elevation model (DEM) to quantitatively study active tectonics. Zhu et al. [18], in this Special Issue, validated the accuracy of the DEMs extracted from GF-7 stereo imagery, with or without ground control points (GCPs), and evaluated the potential of applying GF-7 DEMs to active tectonics. Their study shows that GF-7 can provide large-scale high-resolution topographical and geomorphological data for quantitatively studying active structures. The GCPs extracted from ICESat-2/ATLAS data were used to significantly improve the RMSE values. Using the GF-7 DEMs, the apparent fault scarps and horizontal offsets were effectively identified. Although all three GF-7 DEMs achieved satisfactory accuracy in measuring the horizontal and vertical offsets, the GCPs extracted from ICESat-2/ATLAS data still improved the accuracy of the measurements. This study opens a new path for the application of GF-7 satellite images in seismological research.

Coseismic liquefaction causes great damage to buildings. Coseismic liquefaction refers to the change in sand from a solid state to a liquid state caused by an increase in pore water pressure and a decrease in effective stress following an earthquake [19–21]. The rapid data extraction of the liquefaction caused by strong earthquakes helps assess earthquake intensity and prepare emergency responses. Supervised classification methods are potentially more accurate and do not require pre-earthquake images. However, current supervised classification methods depend on precisely delineated liquefaction polygons using manual and landcover maps. To overcome these shortcomings, Liang et al. [13,14] proposed two binary classification methods based on typical samples. The methods trained two machine learning algorithms with different numbers of typical samples and then used the trained binary classification methods to extract the spatial distribution of the liquefaction. A morphological transformation method was used for the postprocessing of the extracted liquefaction. This study is the first to identify liquefaction based on random forest and gradient boosting decision tree methods with GF satellites. These methods may effectively take advantage of optical satellite images and limited samples in order to quickly identify liquefaction pits after an earthquake.

4. Tectonic and Geomorphic Application of High-Resolution Data Sets

Tectonic geomorphological research is important and uses multisource data to quantify the landscape by recording the geomorphological and tectonic processes. High-resolution data sets are widely used in the field. Liu et al. [1,22] conducted a quantitative analysis of tectonic geomorphological research based on results from the Web of Science from 1981 to 2021. The researchers narrowed their searches according to research areas, countries, institutions, journals, authors, keywords, and citations.

The results show that with the development of remote sensing and tectonic geomorphology and the improvement of instruments and equipment, the amount of research conducted by tectonic geomorphological analysis has been increasing. Via network analyses, the most popular research topics in tectonic geomorphology are as follows: constraining the rates of active faulting and investigating the response of drainage divide migration relative to fault slip rates. These efforts are carried out around the world and are applied rapidly in China, especially in the eastern Tibetan Plateau and in the eastern Chinese Tian Shan. We present some of thess latest researches below.

4.1. Worldwide Tectonic Geomorphological Research Using High-Resolution Data Sets

Constraining the age of formation and the repeated movements along the fault arrays in superimposed rift basins helps us unravel the Earth's kinematic history and the role of inherited structures in basin evolution. Tamas et al. [23] used UAV-based photogrammetry coupled with in situ fieldwork and U–Pb geochronology to decipher multiphase deformation processes in Sarclet, Inner Moray Firth Basin, UK. These findings improve the identification of deformation structures associated with earlier basin-forming events and characterize multiple deformation events. Characteristic structures, fault kinematics, fault rock developments, and associated mineralization types related to these events can all be isolated using these results.

Geological lineaments are linear or curvilinear surfaces that are considered superficial expressions of discontinuities on the Earth's surface. The extraction of lineaments from satellite data is one of the most frequently used applications in remote sensing for geology. Echeverria et al. [24] focused on the semiautomatic extraction of lineaments in the Girón–Santa Isabel basin using a topographic position index. The study provides a new database of lineaments for the basin area that could be useful for developing management and development plans. The methodology in this study can be used to efficiently extract and analyze geological lineaments in large, difficult-to-access regions or those with few outcrops. It allows us to optimize time and reduce costs when collecting structural information on the study area during the first stage of geological, civil, and mining prospecting or in the educational field. Furthermore, it offers a method that combines the automatic extraction of lineaments with the analysis of geospatial data to determine fracture zones or faults.

A drainage divide is a dynamic feature that migrates in response to tectonic activity. The asymmetric uplift between two adjacent basins causes the divide to migrate from a slower to a faster uplift area. Sado Island, Japan, has been affected by southeastward-tilting uplift for ca. 300k years. Sakashita and Endo [25] conducted a digital-elevation-model-based investigation that focused on divide migration. They concluded that the main divides of Sado have presumably continued to slowly migrate toward the area of faster uplift. These divides will likely never overcome the moving geometric center due to the land expansion at the seacoast caused by asymmetric uplift.

4.2. Tectonic and Geomorphic Evolution of the Eastern Tibetan Plateau and the Tian Shan

As the latest boundary of outward plateau expansion, the southern Alashan Block lies the closest to the northeastern Tibetan Plateau. Yabrai Shan is located at the intersection of the Tibetan Plateau, Alashan and Ordos Blocks and records the evolution of surface processes and tectonic activities in the northeastern Tibetan Plateau. Ji et al. [26] conducted a quantitative landform analysis of Yabrai Shan. The spatiotemporal distribution of the geomorphological parameters indicated that Yabrai Shan is in the mature stage of its geomorphological evolution and is controlled by the tectonic activities of the Yabrai range-front fault. Two tectonic acceleration events were identified. Different distribution characteristics of two-phase knickpoints are caused by the change in tectonic stress in this region, revealing that the late knickpoints are the result of tectonic acceleration under the influence of the northeast expansion of the Tibetan Plateau. The transformation of Yabrai Shan from the original extensional environment affected by the Ordos Block to the compressional environment affected by the northeast expansion of the Tibetan Plateau occurred after 1.10 Ma.

The Sichuan–Yunnan rhomboidal block is one of the most complex, deformed, and seismically active regions in mainland China due to the joint action of the northeastward pushing of the Indian Block, the southeastward extrusion of plateau material, and the blocking of the South China Block. Because of the particularity of its location, it has become a key area for researchers to conduct active tectonic and seismic monitoring and prediction [27–33]. The Red River Fault Zone, at the southwestern boundary of the Sichuan–Yunnan rhomboidal block, is an important large-scale fault zone that cuts the Indochina Block and the Yangzi–South China Block in southwestern China, and it is located

at the front of the transverse extrusion and deformation of the Qinghai–Tibet Plateau. It plays a key role in the extrusion, rotation, and escape of continental masses on the southeastern margin of the Qinghai–Tibet Plateau. Based on a digital elevation model and GIS technology, Guo et al. [34] extracted and analyzed the stream geomorphic indices of the northern segment of the Red River Fault Zone. Their results show that the northern segment of the Red River Fault Zone is highly active, that the activity level shows a decreasing trend from north to south, and that the activity in the northern segment has been the most intense since the late Pleistocene.

The Tian Shan is one of the most active intracontinental orogenic belts in the world. Using high-resolution remote sensing photography, the deformation of fluvial terraces, and field-based geological cross-sections, Yang et al. [35] obtained the quaternary crustal shortening of the Houyanshan structure in the eastern Chinese region of the Tian Shan. The shortening rate and total shortening amount suggest that the structure may have formed at 1.8–3.7 Ma, which is nearly synchronous around the Tibetan Plateau. Together, these results indicate that this combined geological and geomorphological analysis provides greater insight into deformation information than can be achieved by any individual technique in studying fold-and-thrust belts worldwide.

5. Concluding Remarks

The collection of papers in this Special Issue represents a diverse suite of the most recent works pertaining to the remote sensing perspectives of geomorphological and tectonic processes. Detailed scientific studies of major earthquake hazards provide an accumulation of valuable experience for the prediction and prevention of earthquake disaster mitigation. The studies of the surface processes of the seismogenic structures involved in major earthquakes using high-resolution data sets help to cultivate a deep understanding of the mechanisms and patterns of earthquake hazards and provide a theoretical basis for earthquake disaster reduction.

New seismological methods using high-resolution data sets broaden the vision of studying active tectonic geomorphological processes. China's first optical stereo mapping satellite with a submeter resolution, GaoFen-7, shows significant potential for providing high-resolution topographic and geomorphic data for quantitative research on active tectonics. Binary classification methods based on machine learning make the automatic identification of liquefaction induced by strong earthquakes feasible. These methods could efficiently and quickly provide a spatial distribution of liquefaction based on post-earthquake emergency satellite images. This will strongly improve our ability to assess earthquake intensity and prepare emergency responses. The case studies from Sarclet, Inner Moray Firth Basin, UK; the Girón–Santa Isabel Basin, South Ecuador; and Sado Island, Japan show the extensive global application of remote sensing perspectives on geomorphological and tectonic processes. High-resolution remote sensing data have been expertly applied to studies on the geomorphic evolution of the Southern Alashan Block of the Northeastern Tibetan Plateau, the piedmont fault activity in the Red River Fault Zone of the southeastern Tibetan Plateau, and the Houyanshan Structure in the Eastern Chinese Tian Shan, as shown in this Special Issue. These applications show the broad prospects of this tectonic research for the Qinghai–Tibet Plateau and its surrounding areas.

References

1. Liu, J.; Ren, Z.; Zhang, H.; Li, C.; Zhang, Z.; Zheng, W.; Li, X.; Liu, C. Slip rates along the laohushan fault and spatial variation in slip rate along the Haiyuan fault zone. *Tectonics* **2022**, *41*, e2021TC006992. [CrossRef]
2. Ren, Z.; Zhang, Z.; Chen, T.; Yan, S.; Yin, J.; Zhang, P.; Zheng, W.; Zhang, H.; Li, C. Clustering of offsets on the Haiyuan fault and their relationship to paleoearthquakes. *GSA Bull.* **2016**, *128*, 3–18. [CrossRef]
3. Ren, Z.; Zhang, Z.; Zhang, H.; Zheng, W.; Zhang, P. The role of the 2008 Mw 7.9 Wenchuan earthquake in topographic evolution: Seismically induced landslides and the associated isostatic response. *Tectonics* **2018**, *37*, 2748–2757. [CrossRef]
4. Ren, Z.; Zielke, O.; Yu, J. Active tectonics in 4D high-resolution. *J. Struct. Geol.* **2018**, *117*, 264–271. [CrossRef]
5. Zhang, P.; Molnar, P.; Downs, W.R. Increased sedimentation rates and grain sizes 2–4 Myr ago due to the influence of climate change on erosion rates. *Nature* **2001**, *410*, 891–897. [CrossRef]
6. Zhang, P.-Z. Beware of slowly slipping faults. *Nat. Geosci.* **2013**, *6*, 323–324. [CrossRef]
7. Zhang, P.-Z.; Shen, Z.; Wang, M.; Gan, W.; Bürgmann, R.; Molnar, P.; Wang, Q.; Niu, Z.; Sun, J.; Wu, J.; et al. Continuous deformation of the Tibetan plateau from global positioning system data. *Geology* **2004**, *32*, 809–812. [CrossRef]
8. Xu, D.; He, Z.; Ma, B.; Liang, K.; Long, J.; Zhang, H. Classification and semiquantitative evaluation of paleoearthquake identification from trenches on normal faults: A case study of holocene paleoearthquake events from the northern margin of the hetao basin, China. *Tectonics* **2023**, *42*, e2022TC007443. [CrossRef]
9. He, Z.; Li, Y.; Li, Y.; Sun, X.; Liu, D.; Ding, R.; Yang, P. The surface process and seismogenic structure of the 2021 Ms 6.1 Biru, Central Tibet earthquake. *Seismol. Res. Lett.* **2022**, *93*, 1976–1991. [CrossRef]
10. He, Z.; Ma, B.; Hao, Y.; Zhao, J.; Wang, J. Surface rupture geomorphology and vertical slip rates constrained by terraces along the wulashan piedmont fault in the Hetao Basin, China. *Geomorphology* **2020**, *358*, 107116. [CrossRef]
11. Li, Z.-M.; Li, W.-Q.; Li, T.; Xu, Y.-R.; Su, P.; Guo, P.; Sun, H.-Y.; Ha, G.-H.; Chen, G.-H.; Yuan, Z.-D.; et al. Seismogenic fault and coseismic surface deformation of the maduo *Ms*7.4 earthquake in Qinghai, China: A quick report. *Seismol. Geol.* **2021**, *43*, 722–737. [CrossRef]
12. Xie, H.; Li, Z.; Yuan, D.; Wang, X.; Su, Q.; Li, X.; Wang, A.; Su, P. Characteristics of co-seismic surface rupture of the 2021 Maduo Mw 7.4 earthquake and its tectonic implications for Northern Qinghai—Tibet plateau. *Remote Sens.* **2022**, *14*, 4154. [CrossRef]
13. Liang, P.; Xu, Y.; Li, W.; Zhang, Y.; Tian, Q. Automatic identification of liquefaction induced by 2021 Maduo Mw7.3 earthquake based on machine learning methods. *Remote Sens.* **2022**, *14*, 5595. [CrossRef]
14. Liang, K.; He, Z.; Jiang, W.; Li, Y.; Liu, Z. Surface rupture characteristics of the Menyuan Ms 6.9 earthquake on January 8, 2022, Qinghai Province. *Seismol. Geol.* **2022**, *44*, 256–278.
15. Li, Y.; Jiang, W.; Li, Y.; Shen, W.; He, Z.; Li, B.; Li, Q.; Jiao, Q.; Tian, Y. Coseismic rupture model and tectonic implications of the January 7 2022, Menyuan Mw 6.6 earthquake constraints from InSAR observations and field investigation. *Remote Sens.* **2022**, *14*, 2111. [CrossRef]
16. Wang, J.; Ding, L.; He, J.; Cai, F.; Wang, C.; Zhang, Z. Research of seismogenic structures of the 2016 and 2022 Menyuan earthquakes, in the Northeastern Tibetan plateau. *Remote Sens.* **2023**, *15*, 742. [CrossRef]
17. Jiao, Q.S.; Jiang, W.L.; Li, Q.; Lai, J.B.; Zheng, Y.; He, Z.T.; Shen, W.H.; Li, Y.S.; Luo, Y.; Zhang, J.F. Rapid emergency analysis of the surface rupture related to the Qinghai Menyuan Ms6.9 earthquake on January 8, 2022, using GF-7 satellite images. *Natl. Remote Sens. Bull.* **2022**, *26*, 1895–1908. [CrossRef]
18. Zhu, X.; Ren, Z.; Nie, S.; Bao, G.; Ha, G.; Bai, M.; Liang, P. DEM Generation from GF-7 satellite stereo imagery assisted by space-borne LiDAR and its application to active tectonics. *Remote Sens.* **2023**, *15*, 1480. [CrossRef]
19. Kramer, S.L. *Geotechnical Earthquake Engineering*; Prentice Hall: Hoboken, NJ, USA, 1996; p. 653.
20. Gihm, Y.S.; Kim, S.W.; Ko, K.; Choi, J.-H.; Bae, H.; Hong, P.S.; Lee, Y.; Lee, H.; Jin, K.; Choi, S.-J.; et al. Paleoseismological implications of liquefaction-induced structures caused by the 2017 Pohang earthquake. *Geosci. J.* **2018**, *22*, 871–880. [CrossRef]
21. Chini, M.; Albano, M.; Saroli, M.; Pulvirenti, L.; Moro, M.; Bignami, C.; Falcucci, E.; Gori, S.; Modoni, G.; Pierdicca, N.; et al. Coseismic liquefaction phenomenon analysis by COSMO-SkyMed: 2012 Emilia (Italy) earthquake. *Int. J. Appl. Earth Obs. Geoinf.* **2015**, *39*, 65–78. [CrossRef]
22. Liu, Z.; Zhou, S.; Yu, H.; Zhang, W.; Guo, F.; Chen, X.; Guo, J. Quantitative analysis of tectonic geomorphology research based on web of science from 1981 to 2021. *Remote Sens.* **2022**, *14*, 5227. [CrossRef]
23. Tamas, A.; Holdsworth, R.E.; Tamas, D.M.; Dempsey, E.D.; Hardman, K.; Bird, A.; Underhill, J.R.; McCarthy, D.; McCaffrey, K.J.W.; Selby, D. Using UAV-based photogrammetry coupled with in situ fieldwork and U-Pb geochronology to decipher multi-phase deformation processes: A case study from sarclet, inner moray firth Basin, UK. *Remote Sens.* **2023**, *15*, 695. [CrossRef]
24. Villalta, E.M.D.P.; Viña, O.A.G.; Larreta, E.; Romero, C.P.; Mulas, M. Lineament extraction from digital terrain derivate model: A case study in the Girón–Santa isabel basin, South Ecuador. *Remote Sens.* **2022**, *14*, 5400. [CrossRef]
25. Sakashita, A.; Endo, N. Mobility and location of drainage divides affected by tilting uplift in Sado Island, Japan. *Remote Sens.* **2023**, *15*, 729. [CrossRef]
26. Ji, T.; Zheng, W.; Yang, J.; Zhang, D.; Liang, S.; Li, Y.; Liu, T.; Zhou, H.; Feng, C. Tectonic significances of the geomorphic evolution in the southern alashan block to the outward expansion of the Northeastern Tibetan plateau. *Remote Sens.* **2022**, *14*, 6269. [CrossRef]
27. Royden, L.H.; Burchfiel, B.C.; King, R.W.; Wang, E.; Chen, Z.; Shen, F.; Liu, Y. Surface deformation and lower crustal flow in Eastern Tibet. *Science* **1997**, *276*, 788–790. [CrossRef] [PubMed]

28. Royden, L.H.; Burchfiel, B.C.; Van Der Hilst, R.D. The geological evolution of the Tibetan plateau. *Science* **2008**, *321*, 1054–1058. [CrossRef] [PubMed]

29. Clark, M.K.; Royden, L.H. Topographic ooze: Building the eastern margin of Tibet by lower crustal flow. *Geology* **2000**, *28*, 703–706. [CrossRef]

30. Shen, F.; Royden, L.H.; Burchfiel, B.C. Large-scale crustal deformation of the Tibetan plateau. *J. Geophys. Res. Solid Earth.* **2001**, *106*, 6793–6816. [CrossRef]

31. Su, Y.; Qin, J. Strong earthquake activity and relation to regional neotectonic movement in Sichuan-Yunnan region. *Earthq. Res. China* **2001**, *17*, 24–34.

32. Xu, X.-X.; Ji, L.-Y.; Zhu, L.-Y.; Wang, G.-M.; Zhang, W.-T.; Li, N. The co-seismic deformation characteristics and seismogenic structure of the yangbi *M*S6.4 earthquake. *Seismol. Geol.* **2021**, *43*, 771–789. [CrossRef]

33. Wan, Y.-K.; Shen, X.-Q.; Liu, R.-F.; Liu, X.; Zheng, Z.-J.; Li, Y.; Zhang, Y.; Wang, L. Present slip and stress distribution of block boundary faults in the Sichuan-Yunnan region. *Seismol. Geol.* **2021**, *43*, 1614–1637. [CrossRef]

34. Guo, L.; He, Z.; Li, L. Responses of stream geomorphic indices to piedmont fault activity in the Northern segment of the red river fault zone. *Remote Sens.* **2023**, *15*, 988. [CrossRef]

35. Yang, X.; Li, Z.; Wang, W.; Zhang, P.; Wu, C.; Chen, G.; Duan, L.; Wu, X.; Liu, K. Quaternary crustal shortening of the houyanshan structure in the Eastern Chinese Tian Shan: Constrained from geological and geomorphological analyses. *Remote Sens.* **2023**, *15*, 1603. [CrossRef]